Pseudomonas syringae pv. *tomato* DC3000 induces defense responses in diverse maize inbred lines

Namrata Jaiswal[1] and Matthew Helm[1] *

[1] Crop Production and Pest Control Research Unit, U.S. Department of Agriculture-Agricultural Research Service (USDA-ARS), West Lafayette, IN 47907, U.S.A.

* **Corresponding author:** M. Helm; Email: Matthew.Helm@usda.gov

Funding

This research was funded by the United States Department of Agriculture, Agricultural Research Service (USDA-ARS) research project 5020-21220-014-00D. The funding bodies had no role in designing the experiments, collecting the data, or writing the manuscript. All opinions expressed in this paper are the author's and do not necessarily reflect the policies and views of USDA. USDA is an equal opportunity provider and employer.

ABSTRACT

Many phytopathogens translocate virulence (effector) proteins into plant cells to circumvent host immune responses during infection. One such pathogen is *Pseudomonas syringae* pv. *tomato* DC3000, which secretes at least twenty-nine effectors into host cells, of which a subset elicits host defense responses in crop plant species. However, it is unknown whether *P. syringae* pv. *tomato* DC3000 activates immune responses in diverse maize inbreds. Here, we screened a diverse maize germplasm collection for effector-dependent recognition of this bacterial pathogen. As a control, we infiltrated *Pseudomonas syringae* DC3000(D36E), a derivative of *P. syringae* pv. *tomato* DC3000 that lacks all endogenous effectors. In our evaluations, we observed a variety of responses to *P. syringae* pv. *tomato* DC3000 in maize and scored the phenotypes as either no observable response (N) or as one of three responses: weak chlorosis (WC), chlorosis (C) with minimal cell death, and hypersensitive reaction (HR)-like cell death. Of the twenty-six maize inbreds screened, 13 were scored as N, 2 as WC, 2 as C, and 9 as HR-like cell death. Importantly, no maize line responded to *P. syringae* DC3000(D36E), demonstrating the responses observed are likely dependent upon recognition of one or more *Pseudomonas* effectors. Importantly, maize inbreds that recognize *P. syringae* pv. *tomato* DC3000 accumulated detectable hydrogen peroxide as well as an increase in transcript expression of a subset of maize defense genes. Collectively, our results will likely stimulate new research aimed at identifying the cognate maize disease resistance proteins that recognize the activities of one or more bacterial effectors.

Key words: maize, *Pseudomonas syringae*, effector delivery, defense responses, ROS

INTRODUCTION

To facilitate disease development, plant phytopathogens often secrete a repertoire of virulence proteins, known as effectors, to host cells during the infection process (Bentham et al., 2020). The primary function of these pathogen-secreted effectors is to manipulate host cell physiology and development, including the structure and function of plant cells as well as modulate host immune responses (Bentham et al., 2020; Lovelace et al., 2023). To circumvent the immune-suppressing activities of diverse plant phytopathogens, plants have evolved a two-tiered, integrated immune signaling network (Bentham et al., 2020; Lovelace et al., 2023; Ngou et al., 2022). The first tier, often referred to as cell surface-triggered immunity, primarily involves the detection of pathogen-associated molecular pattern (PAMPs) by cell surface-localized, transmembrane immune receptors (Bentham et al., 2020; Ngou et al., 2022). Upon recognition of pathogen-derived PAMPs, the host cell will initiate several coordinated defense responses including, in part, an increase in the production reactive oxygen species (ROS), stomatal closure, calcium influx and accumulation within the host cytosol, as well as up-regulation of defense-related genes (Bentham et al., 2020; Chen et al., 2022; Ngou et al., 2022). The second tier of the plant immune system is often mediated by intracellular innate immune receptors known as nucleotide-binding, leucine-rich repeat (NLR) proteins, whose primary function is to detect the activities of pathogen-secreted effectors inside host cells (Bentham et al., 2020; Ngou et al., 2022).

70 Once activated, plant NLR proteins initiate a cell death response, known as the
71 hypersensitive reaction (HR), which is thought to restrict pathogen growth and systemic
72 spread (Bentham et al., 2020; Coll et al., 2011; Ngou et al., 2022). This tier of host
73 immunity is often referred to as effector-triggered immunity (ETI) or intracellular
74 receptor-mediated immunity (Ngou et al., 2022).

75 The bacterial phytopathogen *Pseudomonas syringae* pv. *tomato* DC3000 has
76 been foundational to the study of effector biology and its study has yielded significant
77 insights into the structure of the plant immune system (Wei and Collmer, 2018; Xin and
78 He, 2013). During pathogenesis, this hemibiotrophic pathogen colonizes the host
79 apoplast by entering through stomata and uses the type III secretion system (T3SS) to
80 deliver at least twenty-nine effector proteins directly into the host cell cytoplasm (Wei et
81 al., 2018; Xin and He, 2013). Once translocated, these effector proteins predominantly
82 function to suppress host immune responses or modulate host development, thereby
83 facilitating disease progression (Wei et al., 2018; Xin and He, 2013). For example, the
84 *P. syringae* pv. *tomato* DC3000 effector HopM1 suppresses both PAMP-elicited ROS
85 production as well as stomatal closure in Arabidopsis, thus facilitating disease
86 development (Lozano-Duran et al., 2014). Additionally, the HopK1 effector from *P.*
87 *syringae* pv. *tomato* DC3000 suppresses HR-like cell death elicited by another *P.*
88 *syringae* pv. *tomato* DC3000 effector, HopA1, as well as PTI responses including ROS
89 production and callose deposition (Guo et al., 2009; Jamir et al., 2004; Li et al., 2014).
90 Interestingly, HopK1 encodes a chloroplast transit peptide and accumulates in host
91 chloroplasts, suggesting chloroplast localization may be important for HopK1-mediated
92 suppression of PTI and ETI responses (Li et al., 2014). HopQ1 (also known as HopQ1-

93 1) is conserved across pathogenic bacteria and, intriguingly, induces an HR-like cell
94 death response when transiently expressed in *N. benthamiana* (Ferrante et al., 2009;
95 Wei et al., 2007). Upon *P. syringae* pv. *tomato* DC3000-dependent delivery into
96 Arabidopsis, AvrPto and AvrPtoB function redundantly to attenuate flagellin22 (flg22)
97 perception by the cell surface-localized immune receptor, FLS2 (Boller and Felix, 2009;
98 Kvitko et al., 2009; Martin, 2012).

99 The maize Nested Association Mapping (NAM) recombinant inbred lines (RILs)
100 representing global maize diversity were derived from twenty-six inbred founder lines
101 and are a valuable genetic resource for discovering allelic diversity against plant
102 pathogens of maize (Gage et al., 2020; Singh et al., 2023). For example, Kump and
103 colleagues (2011) used the NAM population to identify thirty-two quantitative trait loci
104 associated with resistance to *Cochliobolus heterostrophus*, the causative pathogen of
105 Southern Leaf Blight disease, in maize. Furthermore, this mapping population was also
106 used to identify the genetic resistance architecture underlying quantitative disease
107 resistance to Gray Leaf Spot (GLS) disease and Northern leaf blight (NLB) disease
108 (Benson et al., 2015; Poland et al., 2011). These studies thus demonstrate the value
109 and versatility of screening the NAM population for identifying maize disease resistance
110 genes. To the best of our knowledge, the maize NAM population has not been used to
111 identify putative sources of genetic resistance to *P. syringae* pv. *tomato* DC3000.

112 In the current study, we screened the maize NAM population for recognition of
113 the bacterial pathogen *P. syringae* pv. *tomato* DC3000. Of the twenty-six maize inbreds
114 evaluated in our screen, 13 were scored as having no observable response to *P.*
115 *syringae* pv. *tomato* DC3000. Two inbred lines were phenotyped as having a weak

116 chlorotic response and two as having a chlorotic response with minimal cell death. The
117 nine remaining maize inbreds all responded to *P. syringae* pv. *tomato* DC3000 with HR-
118 like cell death. Consistent with the phenotypic responses, the maize inbred lines that
119 recognized *P. syringae* pv. *tomato* DC3000 accumulated detectable hydrogen peroxide
120 within the infiltrated regions as well as an increase in transcript expression of a subset
121 of maize defense genes. As a control, we infiltrated an effectorless mutant strain of
122 *Pseudomonas syringae* DC3000, termed *P. syringae* DC3000(D36E), which did not
123 elicit observable defense responses or hydrogen peroxide accumulation in any maize
124 inbred line. These data thus suggest *P. syringae* induces defense responses in diverse
125 maize inbreds and that maize likely encodes disease resistance proteins that recognize
126 the activities of one or more *Pseudomonas* effectors.
127
128
129 **MATERIALS AND METHODS**
130 **Plant growth conditions**
131 Seed of maize inbreds were ordered from the North Central Regional Plant
132 Introduction Station via the National Plant Germplasm System Web Portal. Maize
133 inbreds were grown in plastic pots containing Berger Seed Germination and
134 Propagation Mix supplemented with Osmocote slow-release fertilizer (14-14-14). Plants
135 were maintained in a growth chamber with 16h:8h photoperiod, light:dark at 24°C with
136 light and 22°C in the dark and 60% humidity with average light intensities at plant height
137 of 130µmols/m^2/s.
138

139

140 ***Pseudomonas* growth conditions and leaf infiltration assay**

141 *Pseudomonas syringae* pv. *tomato* DC3000 and *Pseudomonas syringae*
142 DC3000(D36E) strains were grown on King's B (KB) medium supplemented with 25µg
143 of rifampicin and 50µg of kanamycin per milliliter for two days at 30°C. The
144 *Pseudomonas* strains were resuspended in 10mM $MgCl_2$ to an optical density at 600
145 nm (OD_{600}) of 0.5. Bacterial suspensions were infiltrated into the abaxial surface of the
146 second leaf of two-week old maize seedlings using a 1-mL disposable syringe, and the
147 infiltrated regions were indicated with a black permanent marker. The leaf surface was
148 nicked with a sterile razor blade prior to infiltration to facilitate fluid entry. The infiltrated
149 leaves were phenotyped five days following *Pseudomonas* infiltration and a
150 representative leaf was photographed under white light shortly thereafter.

151

152 **Histochemical detection of hydrogen peroxide accumulation**

153 Hydrogen peroxide (one of several reactive oxygen species) accumulation was
154 detected as previously described with slight modifications (Bach-Pages and Preston,
155 2017). Briefly, the *Pseudomonas* suspensions were infiltrated into two-week old maize
156 seedlings and, 3 days post-infiltration, leaf segments were harvested and incubated in
157 freshly prepared 3,3'-diaminobenzidine (DAB) solution (1 mg/mL (Sigma-Aldrich)
158 dissolved in distilled water (pH 3.8) overnight with gentle agitation in the dark. After
159 overnight incubation, the DAB-stained leaf tissues were rinsed with distilled water,
160 submerged in absolute ethanol, and incubated at 65°C for 2 hours to clear the
161 chlorophyll. The leaf segments were rehydrated with 75% ethanol and incubated for 1

162 hour at room temperature, followed by incubation with 50% ethanol until the leaves
163 were cleared of chlorophyll. The cleared leaf tissue was stored in ultrapure water
164 (supplemented with 20% glycerol) for photography. Representative DAB-stained leaf
165 segments were photographed under white light.
166

167 **RNA extraction and reverse transcriptional real-time quantitative PCR of maize**
168 **defense genes**

169 Two-week old maize leaves (cvs. B73 [non-responder] and Mo18W [responder])
170 were infiltrated with *P. syringae* pv. *tomato* DC3000. The infiltrated leaf tissue was
171 harvested 12- and 24-hours post-*Pseudomonas* infiltration, flash frozen in liquid
172 nitrogen, and stored at -80°C until processing. Total RNA was isolated using TRIzol
173 reagent from maize tissues according to the manufacturer's instruction (Direct-zol™
174 RNA miniprep, ZymoResearch) followed by in-column DNase I treatment. RNA
175 concentration was measured using Nanodrop (Thermo Scientific). Two micrograms of
176 total RNA were used for first-strand cDNA synthesis using AMV reverse transcriptase
177 (New England Biolabs). A quantitative real-time PCR (RT-qPCR) assay was performed
178 on a LightCycler 480 II system using 2x SYBR Green qPCR master mix (BioRad).
179 Maize GAPDH (Zm00001eb233140) was chosen as an endogenous reference gene to
180 normalize the data. Three technical replicates of the RT-qPCR assay were used for
181 each sample with a minimum of three biological replicates. Each biological replicate was
182 sampled from three individual plants. The transcript expression level was calculated
183 using the $2^{-\Delta\Delta CT}$ method (Livak and Schmittgen, 2001). The experiment was repeated at
184 least two independent times. Primers used for RT-qPCR are as follows (5' to 3'):

185 ZmGAPDH-FW (CCTGCTTCTCATGGATGGTT); ZmGAPDH-RV
186 (TGGTAGCAGGAAGGGAAACA); ZmPR3-FW (AGCTTCCTCGTCTCATCATCG);
187 ZmPR3-RV (TGTTGACGTAGGCGTAGAGC); ZmPR5-FW
188 (GCAGCCAGGACTTCTACGAC); ZmPR5-RV (CACAGGCATGGGTCTTCAC); ZmPAL-
189 FW (TCTGGTCCCGCTCTCCTACA); ZmPAL-RV (TTGAAGAAGCCGCCCTCGAT);
190 Peroxidase-FW (CTCATCAACCACCCGGACAC); Peroxidase-RV
191 (TGCAGCAAGCCTTATTTGAACA).
192
193
194 **RESULTS**
195 The observation that *P. syringae* pv. *tomato* DC3000 elicits robust immune
196 responses in crop plant species such as wheat led us to hypothesize that this bacterial
197 phytopathogen may also activate defense responses in maize inbreds. To test our
198 hypothesis, we infiltrated the parental inbred lines of the maize nested association
199 mapping population with *P. syringae* pv. *tomato* DC3000 and phenotyped their
200 responses five days post-*Pseudomonas* infiltration (Figure 1A). As a control, we
201 infiltrated *P. syringae* pv. *tomato* DC3000 into wheat leaves, which was previously
202 shown to recognize this bacterial pathogen (Ramachandran et al., 2017). In our
203 evaluations, we observed a variety of responses to *P. syringae* pv. *tomato* DC3000 and
204 scored the phenotypes as either no observable response (N) or as one of three
205 responses: weak chlorosis (WC), chlorosis (C) with minimal cell death, and
206 hypersensitive reaction (HR)-like cell death. Representative examples of phenotypic
207 responses are shown in Figure 1B, and a complete list of inbred lines and their

208 responses are shown in Table 1. Of the twenty-six maize inbreds tested, 13 were
209 scored as N, 2 as WC, and 2 as C (Figure 1B; Table 1). Nine maize inbred lines
210 (CML52, CML69, CML247, CML333, HP301, M162W, Mo18W, Ms71, and IL14H)
211 displayed a HR-like response to *P. syringae* pv. *tomato* DC3000 within the infiltrated
212 region (Figure 1B; Table 1). As a control, we infiltrated a mutant strain of *P. syringae* pv.
213 *tomato* DC3000, termed *P. syringae* DC3000(D36E), which lacks all endogenous
214 bacterial effectors (Carter et al., 2019; Wei et al., 2015). As expected, there was no
215 observable response in any inbred line tested to *P. syringae* DC3000(D36E) (Figure
216 1B). These data thus demonstrate the phenotypic responses observed in response to *P.*
217 *syringae* pv. *tomato* DC3000 are likely dependent upon recognition of one or more *P.*
218 *syringae* effectors.

219 The production and accumulation of reaction oxygen species, including hydrogen
220 peroxide, is often used as a proxy for activation of defense responses (Carter et al.,
221 2019). Therefore, we used 3,3'-diaminobenzidine (DAB) staining following leaf
222 infiltration with either *P. syringae* pv. *tomato* DC3000 or *P. syringae* DC3000(D36E) to
223 test whether the phenotypic responses of some maize inbred lines to *P. syringae* pv.
224 *tomato* DC3000 is correlated with hydrogen peroxide accumulation. Consistent with the
225 phenotypic responses, maize inbreds that displayed an HR-like cell death response to
226 *P. syringae* pv. *tomato* DC3000 accumulated detectable hydrogen peroxide within the
227 infiltrated region (Figure 2). In contrast, there was no hydrogen peroxide detected in
228 maize lines that did not recognize *P. syringae* pv. *tomato* DC3000 or in lines infiltrated
229 with *P. syringae* DC3000(D36E) (Figure 2). These results thus reveal the chlorotic and

230 HR-like cell death response in maize inbreds that recognize *P. syringae* pv. *tomato*
231 DC3000 is strongly correlated with the production and accumulation of ROS.
232 Though chlorotic and cell death responses are considered defense responses in
233 grasses (Carter et al., 2019; Smith and Mansfield, 1981; Yin and Hulbert, 2010), it was
234 unclear whether the *P. syringae* pv. *tomato* DC3000-mediated defense responses in
235 maize were correlated with increased defense gene expression. We, therefore, used
236 reverse transcription-quantitative polymerase chain reaction (RT-qPCR) to measure
237 mRNA abundance of a subset of defense-related maize genes in both non-responding
238 (B73) and a responding (Mo18W) maize inbred lines at 12- and 24-hours post-
239 *Pseudomonas* infiltration. In our analysis, we selected a subset of defense-related
240 maize genes whose transcriptional activation is associated with salicylic acid signaling
241 and which have been previously shown to be up-regulated during maize-pathogen
242 interactions (Przybylska et al., 2018; Shumilaket al., 2023). Consistent with the
243 phenotypic responses to *P. syringae* pv. *tomato* DC3000, transcript expression of the
244 selected defense genes was significantly upregulated in Mo18W when compared to B73
245 at 12- and 24-hours following *Pseudomonas* infiltration (Figure 3). Collectively, these
246 data clearly demonstrate *P. syringae* pv. *tomato* DC3000 activates robust defense
247 responses, including hydrogen peroxide accumulation as well as up-regulation of
248 defense-related genes, in diverse maize inbreds.
249
250
251 **DISCUSSION**

252 Our work presented here is, to the best of our knowledge, the first to show that *P.*
253 *syringae* pv. *tomato* DC3000 elicits HR-like cell death in some maize inbreds.
254 Consistent with our observations, this bacterial pathogen also induces defense
255 responses in both *Nicotiana benthamiana* and soybean via the recognition of the
256 HopQ1-1 and AvrD effectors, respectively (Kobayashi et al., 1989; Wei et al., 2007).
257 Though our work shows that maize recognizes *P. syringae* pv. *tomato* DC3000, it
258 remains unknown which *Pseudomonas* effectors are specifically recognized. To this
259 end, Ruiz-Bedoya and colleagues (2023) recently generated thirty-six coisogenic
260 *Pseudomonas* strains, each expressing a single *Pseudomonas* effector in the
261 effectorless *P. syringae* DC3000(D36E) mutant. Hence, future research efforts will focus
262 on infiltrating the library of *P. syringae* DC3000(D36E) coisogenic strains in maize to
263 determine which bacterial effectors are specifically recognized (Ruiz-Bedoya et al.,
264 2023). Such knowledge will be valuable in determining the molecular and cellular
265 mechanisms underlying nucleotide-binding leucine-rich repeat immune receptors (NLR)-
266 dependent recognition of *P. syringae* pv. *tomato* DC3000 effectors (Prigozhin et al.,
267 2022; Thatcher et al., 2023).
268 The observation that *P. syringae* pv. *tomato* DC3000 elicits defense responses in
269 maize suggests this bacterial pathogen can be utilized as a surrogate for expression of
270 crop pathogen effectors in maize. Indeed, the bacterial type III secretion system from *P.*
271 *syringae* pv. *tomato* DC3000 has been effectively used to deliver candidate effector
272 proteins directly inside host cells to ascertain effector functions (Fabro et al., 2011; Qi et
273 al., 2018; Ramachandran et al., 2017; Sohn et al., 2007). Development of a *P. syringae*
274 pv. *tomato* DC3000-based heterologous expression system in maize will thus likely

275 facilitate the functional screening of effector proteins from obligate biotrophic pathogens
276 of maize. For example, effector proteins from the maize fungal pathogens *Ustilago*
277 *maydis* and *Puccinia polyspora* suppress PAMP-elicited reactive oxygen species
278 production (Chen et al., 2022; Navarrete et al., 2021; Saado et al., 2022). However, it
279 remains unknown whether these crop pathogen effectors are capable of suppressing *P.*
280 *syringae* pv. *tomato* DC3000-mediated defense responses in maize.

281 In summary, we show that *P. syringae* pv. *tomato* DC3000, but not the
282 effectorless mutant, induces robust defense responses in some maize inbreds. Though
283 it is unclear which *P. syringae* pv. *tomato* DC3000 effectors are recognized, our data
284 nevertheless suggests maize likely encodes disease resistance proteins that recognize
285 the activities of one or more *Pseudomonas* effectors. Future research efforts will, in
286 part, focus on fine mapping the genetic loci responsible for *P. syringae* pv. *tomato*
287 DC3000 recognition.

288

289

290 **ACKNOWLEDGEMENTS**

291 We thank the North Central Regional Plant Introduction Station for providing
292 seed of the maize inbred lines and Dr. Terri Cameron (USDA-ARS) for their technical
293 assistance and maintenance of maize germplasm.

294

295

296

297

298

299

300

301 **LITERATURE CITED**

302 **Abramovitch, R.B., Kim, Y.J., Chen, S., Dickman, M.B., and Martin, G.B.** 2003.
303 *Pseudomonas* type III effector AvrPtoB induces plant disease susceptibility by
304 inhibition of host programmed cell death. EMBO J. 22: 60–69.

305 **Bach-Pages, M., and Preston, G.** 2017. Methods to quantify biotic-induced stress in
306 plants. Methods Mol Biol. 1734: 241-255.

307 **Benson, J., Poland, J., Benson, B., Stromberg, E., and Nelson, R.** 2015. Resistance
308 to Gray Leaf Spot of Maize: Genetic Archtecture and Mechansisms Elucidated
309 through Nested Association Mapping and Near-Isogenic Line Analysis. PLoS
310 Genet 11: e1005045.

311 **Bentham, A., De la Concepcion, J., Mukhi, N., Zdrzalek, R., Draeger, M., Gorenkin,**
312 **D., Hughes, R., and Banfield, M.** 2020. A molecular roadmap to the plant
313 immune system. J Biol Chem. 295: 14916-14935.

314 **Boller, T., and Felix, G.** 2009. A renaissance of elicitors: perception of microbe
315 associated molecular patterns and danger signals by pattern-recognition
316 receptors. Annu. Rev. Plant Biol. 60: 379–406.

317 **Carter, M.E., Helm, M., Chapman, A.V.E., Wan, E., Restrepo-Sierra, A.M., Innes,**
318 **R.W., Bogdanove, A.J., and Wise, R.P.** 2019. Convergent evolution of effector
319 protease recognition by *Arabidopsis* and barley. Mol Plant-Microbe Interact. 32:
320 550-565.

321 **Chakravarthy, S., Worley, J.N., Rodriguez-Montes, A., and Collmer, A.** 2018.
322 *Pseudomonas syringae* pv. *tomato* DC3000 polymutants deploying coronatine
323 and two type III effectors produce quantifiable chlorotic spots from individual
324 bacterial colonies in *Nicotiana benthamiana* leaves. Mol Plant Pathol 19: 935-
325 947.
326 **Chen, G., Zhang, B., Ding, J., Wang, H., Deng, C., Wang, J., Yang, Q., Pi, Q.,**
327 **Zhang, R., Zhai, H., Dong, J., Huang, J., Hou, J., Wu, J., Que, J., Zhang, F.,**
328 **Li, W., Min, H., Tabor, G., Li, B., Liu, X., Zhao, J., Yan, J., and Lai, Z**. 2022.
329 Cloning southern rust resistant gene RppK and its cognate gene AvrRppK from
330 Puccinia polyspora. Nat. Commun. 13, 4392.
331 **Chen, J., Zhang, X., Rathjen, J.P., and Dodds, P.N.** 2022. Direct recognition of
332 pathogen effectors by plant NLR immune receptors and downstream signaling.
333 Essays Biochem 66: 471-483.
334 **Coll, N.S., Epple, P., and Dangl, J.L.** 2011. Programmed cell death in the plant
335 immune system. Cell Death Differ. 18: 1247-1256.
336 **Fabro, G., Steinbrenner, J., Coates, M., Ishaque, N., Baxter, L., Studholme, D.J.,**
337 **Körner, E., Allen, R.L., Piquerez, S.J.M., Rougon-Cardoso, A., Greenshields,**
338 **D., Lei, R., Badel, J.L., Caillaud, M.-C., Sohn, K.-H., Van den Ackerveken, G.,**
339 **Parker, J.E., Beynon, J., and Jones, J.D.G**. 2011. Multiple candidate effectors
340 from the oomycete pathogen *Hyaloperonospora Arabidopsis* suppress host plant
341 immunity. PLOS Pathog 7: e1002348.
342 **Ferrante, P., Clarke, C.R., Cavanaugh, K.A., Michelmore, R.W., Buonaurio, R., and**
343 **Vinatzer, B.A.** 2009. Contributions of the effector gene hopQ1-1 to differences in

344 host range between *Pseudomonas syringae pv. phaseolicola* and *P. syringae pv.*
345 *tabaci*. Mol Plant Pathol 10: 837–842.
346
347 **Gage, J.L., Monier, B., Giri, A., and Buckler, E.S.** 2020. Ten Years of the Maize
348 Nested Association Mapping Population: Impact, Limitations, and Future
349 Directions. Plant Cell. 32: 2083–2093.
350 **Giska, F., Lichocka, M., Piechocki, M., Dadlez, M., Schmelzer, E., Hennig, J., and**
351 **Krzymowska, M.** 2013. Phosphorylation of HopQ1, a Type III Effector from
352 *Pseudomonas syringae*, creates a binding site for host 14-3-3 proteins. Plant
353 Physiol 161: 2049–2061.
354 **Guo, M., Tian, F., Wamboldt, Y., and Alfano, J.R.** 2009. The majority of the type III
355 effector inventory of *Pseudomonas syringae pv. tomato* DC3000 can suppress
356 plant immunity. Mol. Plant–Microbe Interact. 22: 1069–1080.
357 **Jamir, Y., Guo, M., Oh, H.-S., Petnicki-Ocwieja, T., Chen, S., Tang, X., Dickman,**
358 **M.B., Collmer, A., and Alfano, J.R.** 2004. Identification of *Pseudomonas*
359 *syringae* type III effectors that can suppress programmed cell death in plants and
360 yeast. Plant J. 37: 554–565.
361 **Kobayashi, D., Tamaki, S., and Keen, N.** 1989. Cloned avirulence genes from the
362 tomato pathogen Pseudomonas syringae pv. tomato confer cultivar specificity on
363 soybean. Proc Natl Acad USA 86: 157-161.
364 **Kump, K., Bradbury, P., Wisser, R., Buckler, E., Belcher, A., Oropeza-Rosas, M.,**
365 **Zwonitzer, J., Kresovich, S., McMullen, M., Ware, D., Balint-Kurti, P., and**
366 **Holland, J.** 2011. Genome-wide association study of quantitative resistance to

367 southern leaf blight in the maize nested association mapping population. Nat
368 Genet. 43: 163-168.
369
370 **Kvitko, B.H., Park, D.H., Velasquez, A.C., Wei, C.-F., Russell, A.B., Martin, G.B.,**
371 **Schneider, D.J. and Collmer, A.** 2009. Deletions in the repertoire of
372 *Pseudomonas syringae pv. tomato* DC3000 type III secretion effector genes
373 reveal functional overlap among effectors. PLoS Pathog. 5: e1000388.
374 **Li, G., Froehlich, J., Elowsky, C., Msanne, J., Ostosh, A., Zhang, C., Awada, T., and**
375 **Alfano, J.** 2014. Distinct Pseudomonas type-III effectors use a cleavable transit
376 peptide to target chloroplast. Plant J 77:310-321.
377 **Li, W., Yadeta, K.A., Elmore, J.M., and Coaker, G.** 2013. The *Pseudomonas* effector
378 HopQ1 promotes bacterial virulence and interacts with tomato 14-3-3 proteins in
379 a phosphorylation dependent manner. Plant Physiol 161: 2062–2074.
380 **Livak, K.J., and Schmittgen, T.D.** 2001. Analysis of relative gene expression data
381 using real-time quantitative PCR and the 2(-delta delta C(T)) method. Methods
382 25: 402-408.
383 **Lovelace, A., Dorhmi, S., Hulin, M., Li, Y., Mansfield, J., and Ma, W.** 2023. Effector
384 identification in plant pathogens. Phytopathology 113: 637-650.
385 **Lozano-Duran, R., Bourdais, G., He, S.Y., and Robatzek, S.** 2014. The bacterial
386 effector HopM1 suppresses PAMP-triggered oxidative burst and stomatal
387 immunity. New Phytol. 202: 259–269.
388 **Martin, G.B.** 2012. Suppression and activation of the plant immune system by
389 *Pseudomonas syringae* effectors AvrPto and AvrPtoB. In: Effectors in Plant–

390 Microbe Interactions (eds F. Martin and S. Kamoun), 123–154 (Wiley-Blackwell,
391 2011).
392
393 **Navarrete, F., Grujic, N., Stirnberg, A., Saado, I., Aleksza, D., Gallei, M., Adi, H.,**
394 **Alcantara, A., Khan, M., Bindics, J., Trujillo, M., and Djamei, A.** 2021. The
395 Pleiades are a cluster of fungal effectors that inhibit host defenses. PLoS Pathog
396 17: e1009641
397 **Ngou, B.P.M., Ding, P., and Jones, J.D.G.** 2022. Thirty years of resistance: Zig-zag
398 through the plant immune system. Plant Cell 34:1447-1478.
399 **Poland, J., Bradbury, P., Buckler, E., and Nelson, R.** 2011. Genome-wide nested
400 association mapping of quantitative resistance to northern leaf blight in maize.
401 Proc Natl Acad Sci USA 108: 6893-6898.
402 **Prigozhin, D., Rangavajjhala, S., and Krasileva, K**. 2022. Majority of the highly
403 variable NLRs in maize share genomic location and contain additional target-
404 binding domains. bioRxiv DOI: https://doi.org/10.1101/2022.10.05.510735
405 **Przybylska, A., Kornobis, F., and Obrepalska-Steplowska, A.** 2018. Analysis of
406 defense gene expression changes in susceptible and tolerante cultivars of maize
407 (Zea mays) upon Meloidogyne arenaria infection. Physiol Mol Plant Pathol 103:
408 78-83.
409 **Qi, M., Grayczyk, J.P., Seitz, J.M., Lee, Y., Link, T.I., Choi, D., Pedley, K.F.,**
410 **Voegele, R.T., Baum, T.J., and Whitham, S.A**. 2018. Suppression or activation
411 of immune responses by predicted secreted proteins of the soybean rust
412 pathogen *Phakopsora pachyrhizi*. Mol Plant-Microbe Interact 31: 163-174.

413 **Ramachandran, S.R., Yin, C., Kud, J., Tanaka, K., Mahoney, A.K., Xiao, F., and**
414 **Hulbert, S.H.** 2017. Effectors from wheat rust fungi suppress multiple plant
415 defense responses. Phytopathology 107: 75-83.
416 **Ruiz-Bedoya, T., Wang, P., Desveaux, D., and Guttman, D.** 2023. Cooperative
417 virulence via the collective action of secreted pathogen effectors. Nat Microbiol 8:
418 640-650.
419 **Saado, I., Chia, K-S., Betz, R., Alcantara, A., Pettko-Szandtner, A., Navarrete, F.,**
420 **D'Auria, J., Kolomiets, M., Melzer, M., Feussner, I., and Djamei, A**. 2022.
421 Effector-mediated relocalization of a maize lipoxygenase protein triggers
422 susceptibility to Ustilago maydis. Plant Cell 34: 2785-2805.
423 **Shumilak, A., El-Shetehy, M., Soliman, A., Tambong, J., and Daayf, F**. 2023. Goss's
424 wilt resistance in corn is mediated via salicylic acid and programmed cell death
425 but not jasmonic acid pathways. Plants 12: 1475.
426 **Singh, R., Shim, S., Telenko, D.E.P., and Goodwin, S**. 2023. Parental inbred lines of
427 the Nested Association Mapping (NAM) population of corn show sources of
428 resistance to tar spot in Northern Indiana. Plant Dis. 107: 262-266.
429 **Smith, J.J., and Mansfield, J.W**. 1981. Interactions between pseudomonads and
430 leaves of oats, wheat and barley. Physiol. Plant Pathol. 18: 345-IN317.
431 **Sohn, K.H., Lei, R., Nemri, A., and Jones, J.D.G.** 2007. The downy mildew effector
432 proteins ATR1 and ATR13 promote disease susceptibility in *Arabidopsis thaliana*.
433 Plant Cell 19: 4077.
434 **Thatcher, S., Jung, M., Panangipalli, G., Fengler, K., Sanyal, A., Li, B., Llaca, V.,**
435 **and Habben, J.** 2023. The NLRomes of Zea mays NAM founder lines and Zea

436 luxurians display presence-absence variation, integrated domain diversity, and
437 mobility. Mol Plant Pathol 24: 742-757.
438
439 **Wei, C-F., Kvitko, B.H., Shimizu, R., Crabill, E., Alfano, J.R., Lin, N.-C., Martin,**
440 **G.B., Huang, H.-C., and Collmer, A.** 2007. A *Pseudomonas syringae pv. tomato*
441 DC3000 mutant lacking the type III effector HopQ1-1 is able to cause disease in
442 the model plant *Nicotiana benthamiana*. Plant J. 51: 32–46.
443 **Wei, H.-L., Chakravarthy, S., Mathieu, J., Helmann, T.C., Stodghill, P., Swingle, B.,**
444 **Martin, G.B. and Collmer, A**. 2015. *Pseudomonas syringae pv. tomato* DC3000
445 type III secretion effector polymutants reveal an interplay between HopAD1 and
446 AvrPtoB. Cell Host Microbe 17: 752–762.
447 **Wei, H-L., and Collmer, A.** 2018. Defining essential processes in plant pathogenesis
448 with *Pseudomonas syringae* pv. *tomato* DC3000 disarmed polymutants and a
449 subset of key type III effectors. Mol Plant Pathol 19: 1779-1794.
450 **Xin, X-F., and He, S.Y.** 2013. Pseudomonas syringae pv. tomato DC3000: a model
451 pathogen for probing disease susceptibility and hormone signaling in plants.
452 Annu Rev Phytopathol 51: 473-498.
453 **Yin, C., and Hulbert, S**. 2010. Prospects for functional analysis of effectors from cereal
454 rust fungi. Euphytica 179: 57-67.
455
456
457
458

459

460

461

462 **FIGURE LEGENDS**

463

464 **Figure 1. *Pseudomonas syringae* pv. *tomato* DC3000 induces defense responses**
465 **in maize. A)** Schematic diagram of the *Pseudomonas* HR assay. The *P. syringae* pv.
466 *tomato* DC3000 and *P. syringae* DC3000(D36E) strains were resuspended in 10mM
467 $MgCl_2$. The bacterial suspensions were adjusted to an optical density at 600nm (OD_{600})
468 of 0.5 and syringe-infiltrated into the underside surface of the second leaf (L2) of two-
469 week old maize seedlings. The infiltrated regions were marked with a black permanent
470 marker. **B)** Responses of the maize inbred lines to either *P. syringae* pv. *tomato*
471 DC3000 or *P. syringae* DC3000(D36E) were phenotyped five days following infiltration.
472 Responses were scored as N, no observable response; WC, weak chlorosis; C,
473 chlorosis with cell death; and HR, hypersensitive reaction. Wheat cv. Fielder inoculated
474 with either *P. syringae* pv. *tomato* DC3000 or *P. syringae* DC3000(D36E) was used as a
475 control (Carter et al., 2019; Ramachandran et al., 2017).

476

477 **Table 1. Responses of the twenty-six inbred maize lines of the nested association**
478 **mapping (NAM) to *Pseudomonas syringae* pv. *tomato* DC3000.** Accession numbers,
479 origins, and market class were mined from the Maize Genetics and Genomics
480 Database.

481

482 **Figure 2: Maize lines accumulated detectable hydrogen peroxide in response to**
483 ***P. syringae* pv. *tomato* DC3000.** Representative maize inbreds assayed and
484 *Pseudomonas* treatments were as in Figure 1B. Three days following *Pseudomonas*
485 infiltration, leaf segments were harvested from the infiltrated regions and stained
486 overnight with 3,3'-diaminobenzidine (DAB) solution. After overnight incubation, the leaf
487 tissue was rinsed with deionized water, cleared with ethanol to remove the chlorophyll,
488 and stored in ultrapure water (supplemented with 20% glycerol) for photography. Wheat
489 cv. Fielder inoculated with either *P. syringae* pv. *tomato* DC3000 or *P. syringae*
490 DC3000(D36E) was used as a control.
491
492 **Figure 3: *P. syringae* pv. *tomato* DC3000 significantly increases transcript**
493 **expression of maize defense genes.** Reverse transcription-quantitative polymerase
494 chain reaction (RT-qPCR) expression analyses of selected maize defense genes:
495 Pathogenesis-related 3 (ZmPR3), Pathogenesis-related 5 (ZmPR5), Phenylalanine
496 Ammonia Lyase (ZmPAL), and peroxidase in response to *P. syringae* pv. *tomato*
497 DC3000. Two-week old maize leaves (cvs. B73 [non-responder] and Mo18W
498 [responder]) were infiltrated with *P. syringae* pv. *tomato* DC3000. The infiltrated leaf
499 tissue was harvested 12- and 24-hours post-*Pseudomonas* infiltration, flash frozen in
500 liquid nitrogen, and stored at -80°C until processing. Total RNA extraction followed by
501 cDNA preparation and expression of defense genes was quantified by RT-qPCR.
502 Values represent mean ± S.D. (n = 3) from three biological replicates and three technical
503 replicates in each experiment. The maize GAPDH gene was used as an internal
504 reference gene. The gene expression in B73 plants at 12 hours after *P. syringae* pv.

505 *tomato* DC3000 infiltration was set to 1. Multiple comparisons were conducted by two-
506 way ANOVA followed by the Šídák's method. One asterisk (*) indicates P<0.05, two (**)
507 P<0.01, three (***) P<0.001, and four (****) P<0.0001.

508 **Figure 1**

A

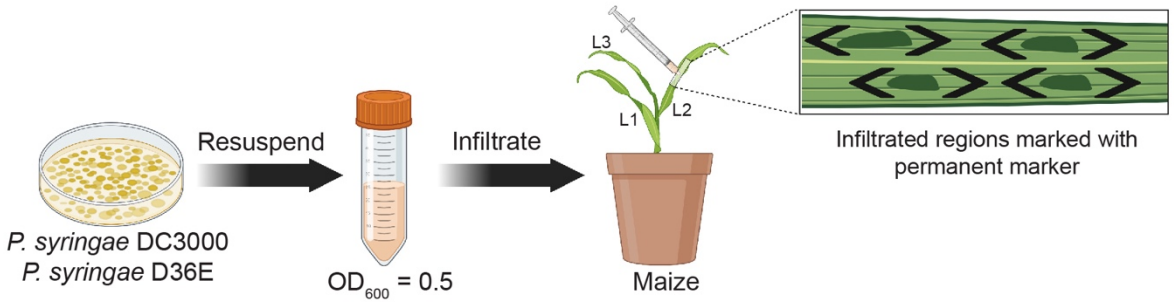
Resuspend
Infiltrate
L3
L1
L2
Infiltrated regions marked with permanent marker
P. syringae DC3000
P. syringae D36E
OD600 = 0.5
Maize

B

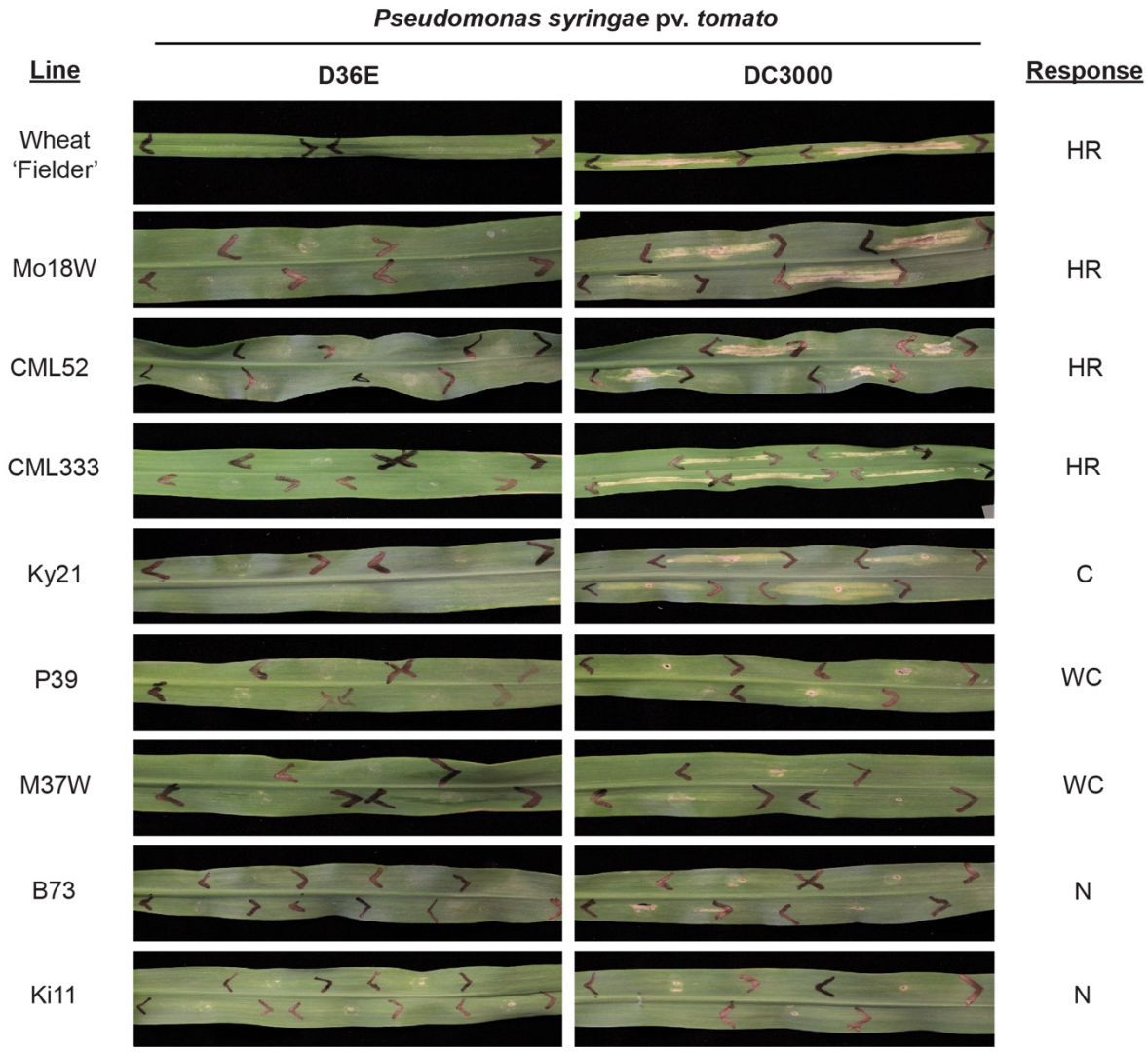
Pseudomonas syringae pv. tomato
Line
D36E
DC3000
Response
Wheat 'Fielder'
HR
Mo18W
HR
CML52
HR
CML333
HR
Ky21
C
P39
WC
M37W
WC
B73
N
Ki11
N

Table 1

Line[a]	Accession	Origin	Market Class	Response[b]
CML52	PI 595561	Ciudad de Mexico, Mexico	Yellow flint	HR
CML69	PI 690318	Ciudad de Mexico, Mexico	Yellow dent	HR
CML247	PI 595541	Ciudad de Mexico, Mexico	White dent	HR
CML333	PI 690322	Ciudad de Mexico, Mexico	White flint	HR
HP301	PI 587131	Indiana, United States	Popcorn	HR
M162W	PI 690328	KwaZulu-Natal, South Africa		HR
Mo18W	PI 550441	Missouri, United States	White dent	HR
Ms71	PI 587137	Michigan, United States		HR
IL14H	PI 690323	Illinois, United States	Sweetcorn	HR
CML277	PI 595550	Ciudad de Mexico, Mexico	White flint	C
Ky21	PI 690326	Kentucky, United States	White dent	C
P39	PI 587133	Indiana, United States	Sweetcorn	WC
M37W	PI 690327	KwaZulu-Natal, South Africa		WC
B73	PI 550473	Iowa, United States	Yellow dent	N
B97	PI 564682	Iowa, United States	Yellow dent	N
CML103	PI 690319	Ciudad de Mexico, Mexico	White dent	N
CML228	PI 690320	Ciudad de Mexico, Mexico	Yellow flint	N
CML322	PI 690321	Ciudad de Mexico, Mexico	White flint	N
Ki3	PI 690324	Thailand	Yellow flint	N
Ki11	PI 690325	Thailand		N
NC350	PI 690329	North Carolina, United States		N
Oh7B	PI 690331	Ohio, United States		N
Oh43	PI 690332	Ohio, United States	Yellow dent	N
Tx303	PI 690334	Texas, United States	Yellow dent	N
Tzi8	PI 506246	Oyo, Nigeria	White flint	N
NC358	PI 690330	North Carolina, United States		N

a Parental inbred lines from the maize Nested Association Mapping (NAM) population.
b Maize leaves (L2) of 14-day-old plants were infiltrated, using a needleless syringe, with a *P. syringae pv. tomato* DC3000 suspension at an optical density at 600 nm (OD_{600}) of 0.5 and photographed 5 days post-infiltration (5dpi). Phenotypes were scored as: N, no ressponse; WC, weak chlorosis; C, chlorosis; and HR, hypersensitive reaction.

Figure 2

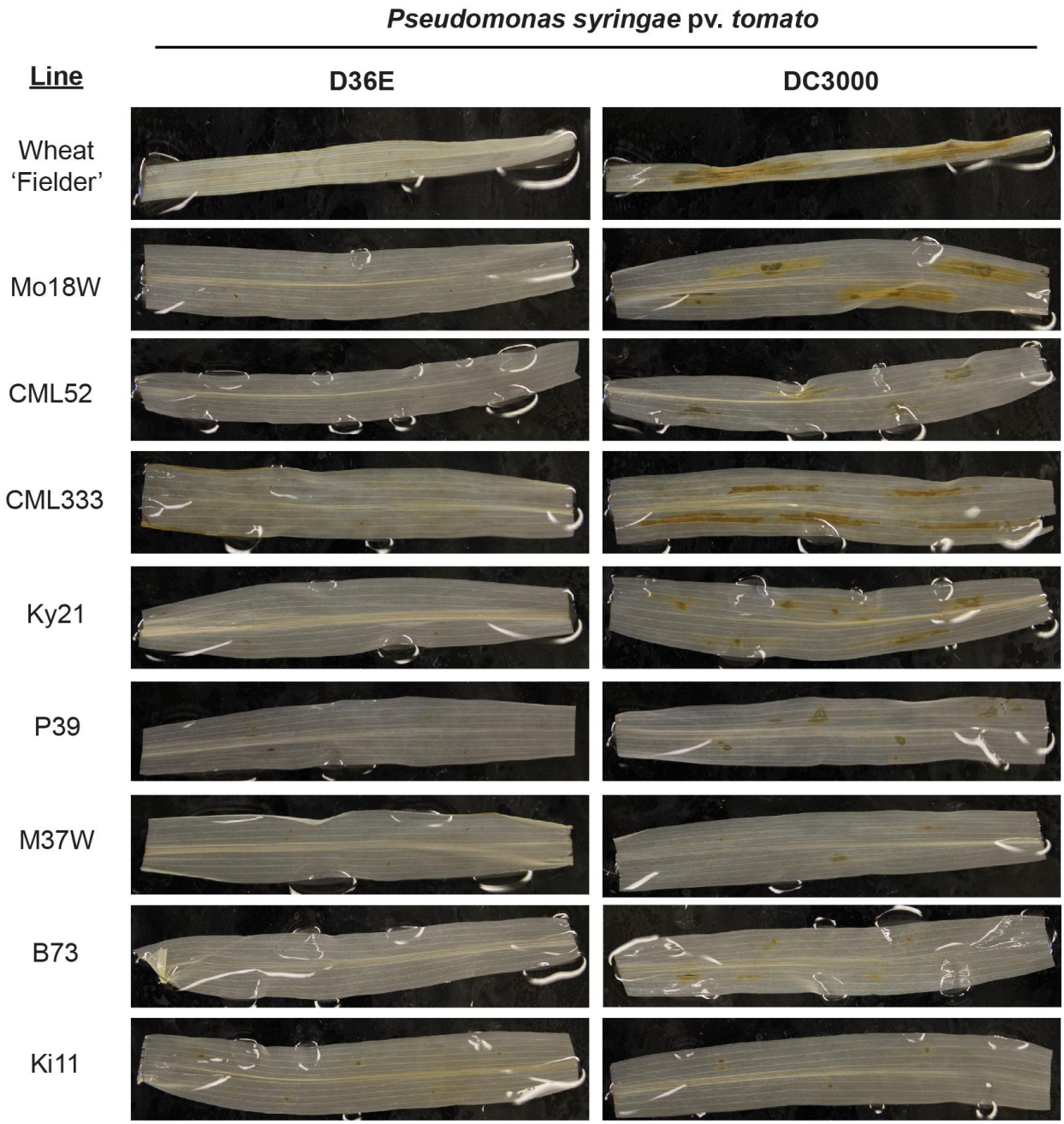

525

526

527

528

529

530 **Figure 3**

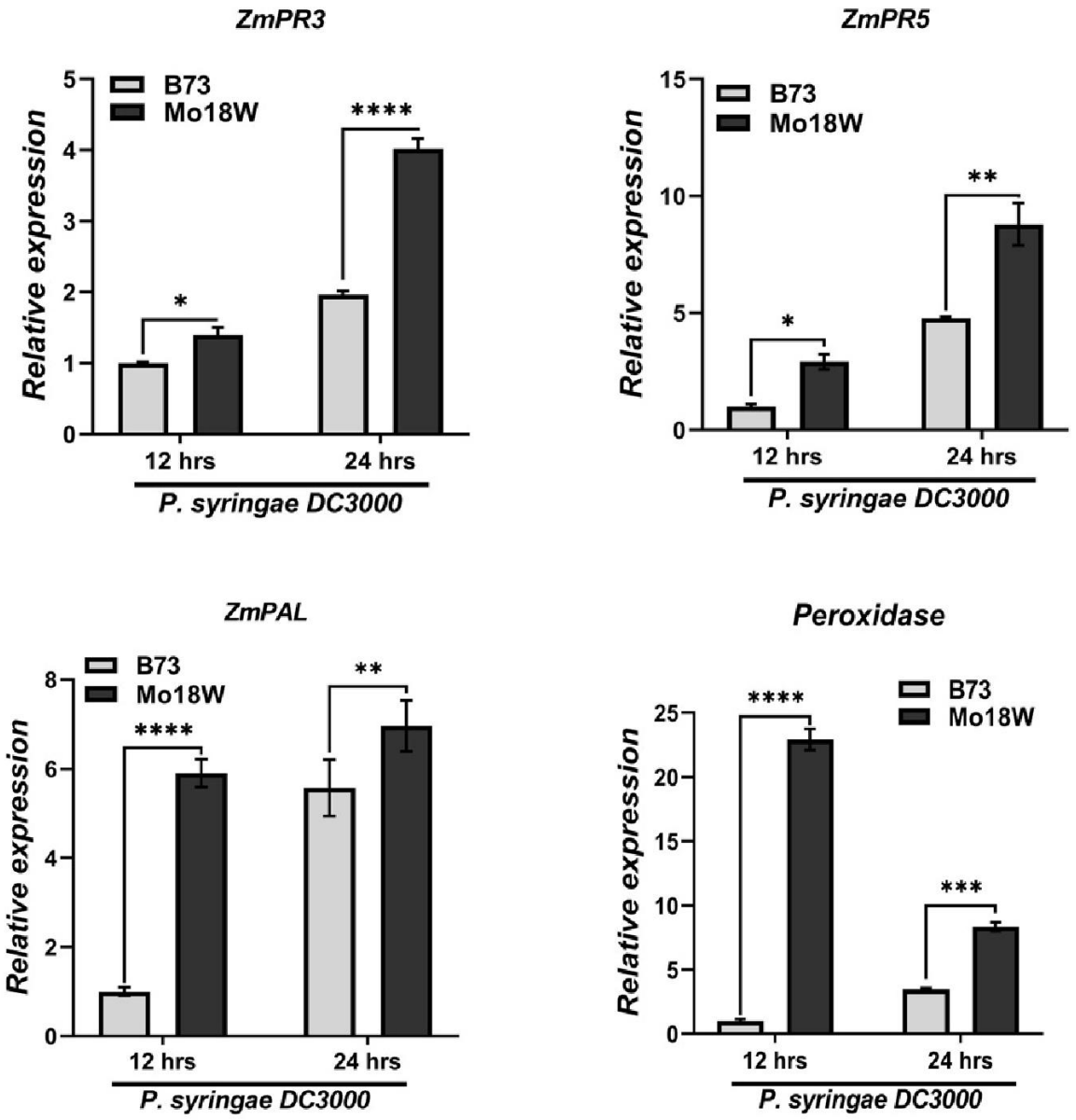
ZmPR3
B73
Mo18W
Relative expression
0
1
2
3
4
5
*
****
12 hrs
24 hrs
P. syringae DC3000
ZmPR5
B73
Mo18W
Relative expression
0
5
10
15
*
**
12 hrs
24 hrs
P. syringae DC3000
ZmPAL
B73
Mo18W
Relative expression
0
2
4
6
8
****
**
12 hrs
24 hrs
P. syringae DC3000
Peroxidase
B73
Mo18W
Relative expression
0
5
10
15
20
25
****
***
12 hrs
24 hrs
P. syringae DC3000

531